Design Approach of Multibeam Using Phased Array Antenna Aided with Butler Matrix for a Fixed Coverage Area

Tumma D. Vani[1, *] and Konidala R. Subhashini[2]

Abstract—This paper devises a framework of phased array antennas to radiate multiple beams for a fixed coverage. The phased antenna array is chosen so that the beamforming can be fixed in selected coverage area. The antenna arrays are employed with a Butler matrix (BM) to form required phases of excitation coefficients to the radiating elements. Optimally designed 4×4 or 8×8 Butler matrix is utilized at the I/O ports of the phased antenna array. The grating lobes are reduced by using the principle of orthogonality to the feeds of subarray (group of column arrays of phased array). This article also exploits the concept of skirt elements to reach the desired coverage area while reducing the beam overlapping in the restricted area. Simulation studies highlight the proposed claims with elaborated numerical analysis of different case studies.

1. INTRODUCTION

The phased array antennas [1–6] are designed for high gain that can serve higher frequencies and improved phase progression technology. This technology enables sharp radiation patterns and steering antenna array beams toward a desired direction by using a phased array antenna. This paper presents the realization of multiple beams using the phased array antenna. In this implementation, an array of $M \times N$ is employed, where M represents number of elements in each linear array, and N represents number of linear arrays. To improve the design of phased array antennas, a passive Butler matrix (BM) [7–11] beamforming feed network is used. The theoretical foundations for the implementation of using BM are developed for the general multibeam realization, which allows one to define a relatively arbitrary coverage domain. It overcomes the restriction of a conventional BM approach by distributing the beams over the fixed angular region instead of over the entire front half-space. The phased array antenna is grouped into subarrays to provide multiple beamforming circuits. A more serious problem is decreased aperture efficiency, due to the requirement that the multiple beams cross over at very high level. To address this problem, a skirt element theory is appended in order to keep intact the efficiency and beam overlap, which is the main objective of the proposed method. Literature suggests that the most successful applications are in the satellite DTV (Direct Television) receptions, where the reflector antennas are widely employed to realize the concepts using multiple offset feeds [12–17]. In this case, the radiations of reflector antennas, when it is illuminated by each feed, are highly directive with their main beams pointing to different satellites. Multiple-beam antennas are currently being used for Direct-Broadcast Satellites (DBS) and Personal Communication Satellites (PCS). These antennas provide mostly contiguous coverage over a specified field of view on earth by using high-gain multiple spot beams for coverage. The multibeam antennas with multiple beam selection ports are implemented through optical antennas which are huge. Their overall sizes have made them unpractical in the ground communications especially in the low frequency bands. Low profile antennas realized using planar phased array antennas become more attractive for they need a smaller space to install and can be integrated with

* Corresponding author: Tumma Divya Vani (tummadivya479@gmail.com).
[1] Department of Electrical Engineering, National Institute of Technology, Rourkela, India. [2] Department of Electrical Engineering, National Institute of Technology, Rourkela, India.

many environmental structures. Literature suggests that there will be a little amount of phase errors, which affect the return losses of the antenna array operating at a fixed frequency [25–27, 33]. Another aspect is the choice of materials that would affect the size and insertion loss of a Butler matrix [28–32]. This paper is organized into four major sections. Section 2 is concerned with the method of realization of set of beams from a phased array. In Section 3, the design approach for the proposed objectives such as coverage area and multiple beams using BM are explained. In Section 4, the application of skirt elements for beamwidth and beam overlapping area control are presented. Section 5 elaborates simulation for different case studies with supporting numerical analysis. Finally, Section 6 gives the conclusion of this paper with future scope. The nomenclature of various parameters is given in Table 1, and this nomenclature is maintained same throughout the article.

Table 1. Nomenclature.

d_x	Distance between two column (linear array) arrays along x axis
d_y	Distance between two antenna elements along y axis
BM	Butler Matrix
BFC	Beam Forming Circuits
DFT	Discrete Fourier Transform
N	Number of elements in each column (linear) array
M	Total number of column arrays
Q	Number of directional beams
$\bar{E}_{mn}$	Elemental radiation pattern
$\bar{E}$	Field basis function of a linear array
ψ	Linear phase excitation from BM
Ω	Angular span
M_s	Number of subarrays
G_{norm}	Normalized gain
M_{sk}	Number of skirt elements

2. MATHEMATICAL MODELING OF MULTIBEAM

The system for realization of multiple beams using phased array antenna with feeding system Butler matrix is as shown in Figure 1. The antenna system for multibeam radiations consists of a 2-D array of identical elements spaced by the equal distances d_x and d_y in x-D and y-D, respectively, as illustrated
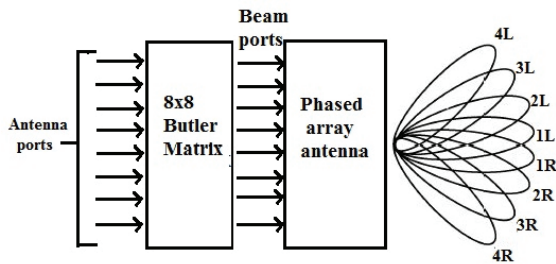

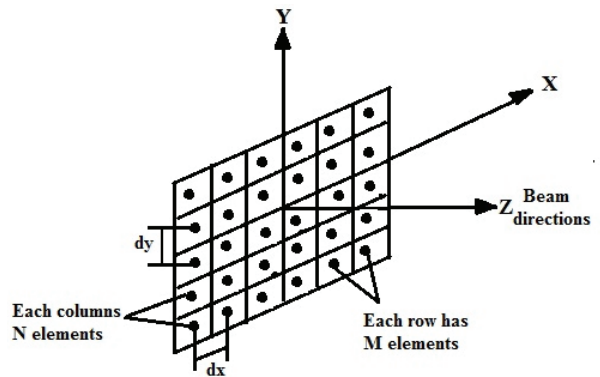**Figure 1.** Block diagram of the multi beam setup.

Figure 2. Antenna arrangement in plane for multibeam radiation.

in Figure 2. A group of N elements in vertical dimension are considered as a single conventional uniform array. Like this we have M columns (linear array) arrays along horizontal dimension with d_x as a spacing between two columns (linear array) arrays. These linear columns arrays are excited by independent BFC feeding system [18] core as a Butler matrix as shown in Figure 3.
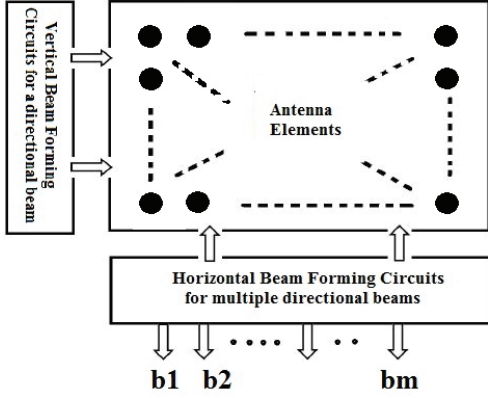

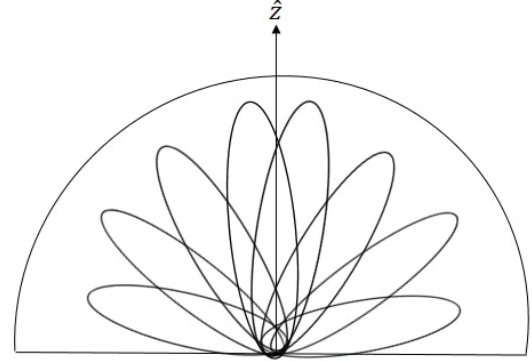**Figure 3.** Systematic design for the multibeam radiation.

Figure 4. Directional beams expansion in $+z$ half space in x-z plane.

2.1. Field Realization of Single Antenna Element

The antenna elements in each column (linear array) are electrically small and radiate electromagnetic fields with a linear polarization in X-axis. The radiated field of each element is represented by a method of cosine tapers [19], which gives closed-form expressions for the directivity of a planar array with arbitrary element locations and excitation identical patterns approximated by cosine functions, identical orientations and polarizations [2]. The elemental radiation $\bar{E}_{mn}(\bar{r})$ of the mn^{th} element located at $\bar{r}' = (x'_{mn}, y'_{mn}, 0)$ is modelled by Equation (1)

$$\bar{E}_{mn}(\bar{r}) = \bar{G}(\theta_{mn}, \phi_{mn})\frac{e^{-jkr_{mn}}}{r_{mn}} \tag{1}$$

where $\bar{r}_{mn} = \bar{r} - \bar{r}'_{mn}$ with $\bar{r}'_{mn} = (r_{mn}, \theta_{mn}, \phi_{mn})$ and $\bar{r} = (r, \theta, \phi)$ in the spherical coordinate system. In Equation (1), $G(\theta_{mn}, \phi_{mn})$ is the individual elemental radiation function, which is modeled by cosine tapers [12].

$$\bar{G}(\theta_{mn}, \phi_{mn}) = \left[\widehat{\theta}_{mn} \cos^{t_1}\theta_{mn}\cos\phi_{mn} - \widehat{\phi}_{mn}\cos^{t_2}\theta_{mn}\sin\phi_{mn}\right], \ 0 \le \theta \le \pi/2 \tag{2}$$

The above equation is defined for x polarized element. The radiation pattern for the y polarized element is also given in [19]. The shape of the radiation pattern is controlled by indices (t_1, t_2). These values are obtained by equating Equation (2) to the actual elements radiation pattern obtained from either experimental measurements or by numerical simulations [19].

2.2. Total Field Pattern of Multiple Beams

The design methodology of the multibeam is explained in Figure 3. The radiation pattern of each column (linear array) array is served as a field basis function for horizontal beamforming circuits [20, 21] to form a multibeam. Thus the net field of the βth beam is given by Equation (3)

$$\bar{E}_{\beta}(\bar{r}) = \sum_{m=1}^{M} B_m e^{j\varphi_{\beta m}}\bar{E}_m^{\text{c}}(\bar{r}) \tag{3}$$

where $\bar{E}_m^c(\bar{r})$ is the field basis function of the mth column array, which is given by Equation (4).

$$\bar{E}_m^c(\bar{r}) = \sum_{n=1}^{N} A_{mn} e^{j\phi_{mn}} \bar{E}_{mn}(\bar{r}) \tag{4}$$

In Equation (3), B_m and $\varphi_{\beta m}$ are amplitudes and phase excitations of βth beam, obtained by BM. A_{mn} and ϕ_{mn} are amplitude and phase excitations of the column (linear) array field equation given in Equation (4). The vertical BFC blocks are used to generate the field basis function for multibeam synthesis from the elemental radiation patterns. And the horizontal BFC blocks are for multibeam synthesis as shown in Figure 3. Beam forming circuits are used to achieve directional signal transmission. To change the directionality of the array while transmitting, a beam former can control the phase and relative amplitude of the beam at each column (linear array) array. The Q multiple beams are formed from M antenna ports by grouping the Q antenna ports into a single subarray.

3. DESIGN APPROACH

The generalized approach to form Q directional beams from a whole group of the M antenna array by the concept of subarray decomposition is explained in this section.

3.1. Subarray Decomposition

A linear column array along the vertical dimension is formed by grouping the N antenna elements with spacing dy between them. Thus M column arrays (total number of columns) are formed along the horizontal dimension with a spacing of dx between them as shown in Figure 2. These column (linear array) arrays along the horizontal dimension are subdivided into L subarrays with each subarray of Q column arrays to form Q beams in the horizontal angular span. The columns in the subarray are periodically arranged. The net radiation field from the bth subarray can be given by Equation (5).

$$\bar{E}_\beta^b = \sum_{q=0}^{Q-1} e^{j\varphi_{\beta q}^b} E_q^{c,b}(\bar{r}) \tag{5}$$

where superscript b indicates b^{th} subarray with its implication using a BM; c indicates the column array; subscript q indicates the subarray number; β indicates the βth beam. Equation (5) is similar to Equation (3) by putting $B_m = 1$. Finally, $\varphi_b^{\beta q}$ indicates linear phase from BM to excite each column (linear array) array.

This is implemented by a Butler matrix concept. BM is a passive electrical network mechanism similar to DFT algorithm. So it is an effective method of feeding multiple beams. Discrete Fourier Transform (DFT) mechanism results in uniform amplitudes and linear phase variations for excitations, and has an equal number of input and output ports. The Q directional beams are formed by using a $Q \times Q$ BM matrix. The Q directional beams are orthogonal to each other. The phase excitations to the subarray fed by BM are given in Equation (5). The linear phase excitations from BM [22] are given by

$$\left.\begin{aligned} \varphi_{\beta q}^b &= \psi_q^\beta + \Delta\varphi_q^b, \\ \psi_q^\beta &= 2\pi\frac{\beta(q+1)}{Q} \end{aligned}\right\} \tag{6}$$

The first term in Equation (6) is the DFT liner phase obtained from BM. The second term is the phase error, which is neglected in practice. To analyse radiation characteristics of the array, one can assume that the selected Q columns of the subarray are identical with a spacing of d_x^b, which is different from the normal elemental spacing d_x. Using Equation (5) and Equation (6) we can write the equation below to get the radiation characteristics of the subarray.

$$\bar{E}_\beta^b = E_0^{c,b}(\bar{r}) \sum_{q=1}^{Q-1} e^{j\Delta\varphi_q^b} e^{j2\Pi\frac{\beta(q+1)}{Q}} e^{jkqd_x^b} \tag{7}$$

In Equation (7), the term $E_0^{c,b}(\bar{r})$ is first column, which is common term to each subarray due to the identical column arrays of equal spacing. If the phase error $\Delta\varphi_q^b$ term is neglected, then the maximum beam direction occurs at,

$$\left.\begin{array}{l} \sin\theta_{peak}^p = -\dfrac{1}{d_x^b/\lambda}\left(\dfrac{\beta}{Q}+p\right) \\[3mm] = \sin\theta_{peak}^0 - \dfrac{p}{d_x^b/\lambda} \end{array}\right\} \tag{8}$$

Here p indicates an integer index to represent grating lobe direction. $p = 0$ indicates the main beam direction, which is given by,

$$\sin\theta_{peak}^0 = -\dfrac{1}{d_x^b/\lambda}\dfrac{\beta}{Q} \tag{9}$$

where Equations (8) and (9) are used to represent the directions of grating lobe and main beam, respectively. The beamwidth of main beam can be calculated from the beam overlapping intersection point, which is obtained by Equation (9).

$$\Delta\sin\theta_{peak}^0 = \lambda/Qd_x^b \tag{10}$$

However, the grating lobe may affect the radiation in the given space due to $d_x^b > \lambda/2$, and this larger value will make main bemas expand at boundary.

3.2. Coverage Domain Analysis

The entire front half space x-z plane is the coverage domain for the multiple beams as shown in Figure 4. These Q beams are uniformly distributed in the xz plane when $d_x^b \leq \lambda/2$ as shown in Figure 4. If $d_x^b > \lambda/2$ then front half space is covered by multiple beams with grating lobes as shown in Figure 5. Since the coverage area is small, the grating lobes are out of coverage, so it is very difficult to eliminate them by terminating unwanted ports, as shown in Figure 6, which will increase the complexity of BFC.

If the given coverage area is arbitrarily small, it will become very difficult to get the main beam direction with in the given angular span. For a larger coverage the beam expansion (Q is more) in the given angular span is obtained with grating lobes outside the region, and it is easy to ignore the grating lobes out of region in this case. In order to get the flexibility in the coverage domain, it is needed to employ the flexible design of the antenna elements in terms of the arbitrary directional multiple beams. In this paper we have taken a arbitrarily large coverage area which supports more directional beams such that complexity in smaller areas get eliminated. The coverage domain is defined by a parameter angular span Ω. The deigned Q directional beams are expected to orthogonally overlap in the given
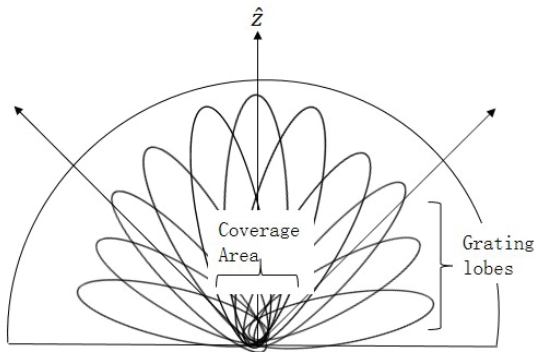

Figure 5. Grating lobes out of coverage area when $d_x^b > \lambda/2$.
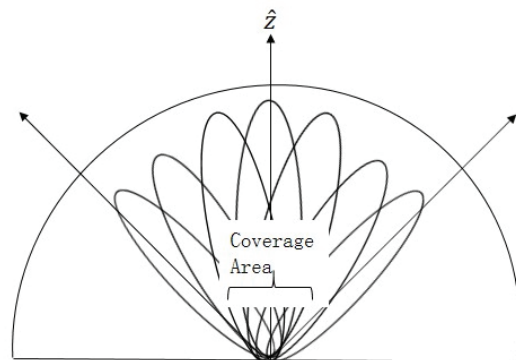
Figure 6. Main beams expansion in desire coverage area.

angular span as shown in Figure 6, where grating lobes do not appear. The angular separation between the two adjacent beams, i.e., $\beta + 1^{\text{th}}$ and β^{th} excluding grating lobes is given by Equation (11).

$$\Theta_s = |\sin\theta^p_{peak}|_{\beta\pm1} - |\sin\theta^p_{peak}|_{\beta} = \frac{1}{(d^b_x/\lambda)Q} \tag{11}$$

From above equation it is clearly observed that the angular separation is inversely proportional to the separation d^b_x. This equation is also used to evaluate the separation of grating lobes between each pair of adjacent beams. A larger value of the d^b_x results in more grating lobes, which is a difficult problem in smaller coverage case. The total number of M column arrays (linear arrays) are decomposed into $M_s = M/Q$ subarrays, where Q is the number of column arrays in each subarray and also the number of directional beams, and M_s is the number of subarrays. Each subarray as shown in Figure 7 is analysed in a way as described in Subsection 3.1. The interleaved arrangement of elements in subarray is employed instead of consecutive arrays in this paper as shown in Figure 7 (this figure is set up for eight beam generation, in the case of four beams replace eight linear arrays by four linear arrays). In Figure 7, three subarrays are shown with different colors with b indicating the subarray number and ϕ^b_β the linear phases from a feeding network BM where the spacing between the elements of the subarray is $d^b_x = 7d_x$, which is larger than the wavelength and leads to more grating lobes. The mechanism of subarray decomposition is employed to linearly combine the subaarays to form multiple directional beams with the same BM ports, which results in cancelation of the grating lobes out of coverage domain. This is the advantage of the lager coverage area compared to smaller areas.
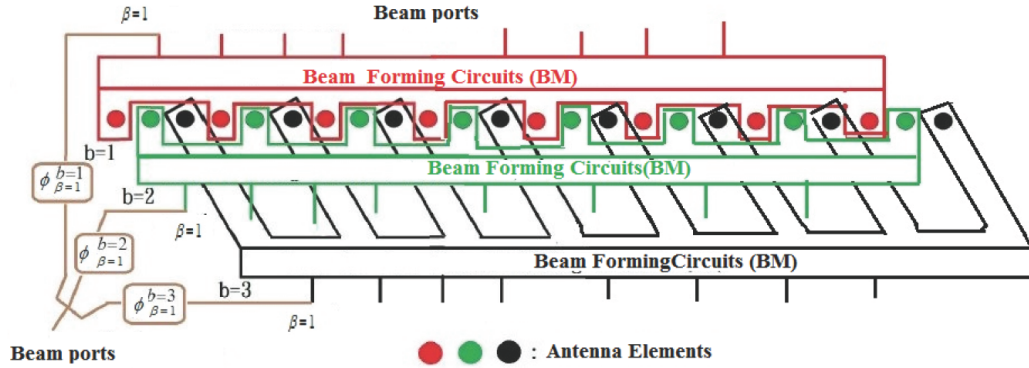

Figure 7. Subarray decomposition using the interleaved elements arrangement.

Table 2. Phase distribution of a 8×8 Butler matrix feed.

Beam port/Ant port	A1	A2	A3	A4	A5	A6	A7	A8	Phase diff (deg)	Beam angle (deg)
1L	90	−180	157.5	−112.5	135	−135	157.5	−112.5	22.5	−7
4R	−180	22.5	−135	67.5	−90	112.5	−45	157.5	−157.5	61
3L	157.7	−90	22.5	135	−112.5	0	112.5	−135	112.5	−39
2R	−112.5	−180	112.5	45	−22.5	−90	−157.5	135	−67.5	22
2L	135	−157.5	−90	−22.5	45	112.5	−150	−112.5	67.5	−22
3R	−135	112.5	0	−112.5	135	22.5	−90	157.7	−112.5	39
4L	157.5	−45	112.5	−90	67.5	−135	22.5	−180	157.5	−61
1R	−112.5	157.5	−135	135	−112.5	157.5	−180	90	−22.5	7
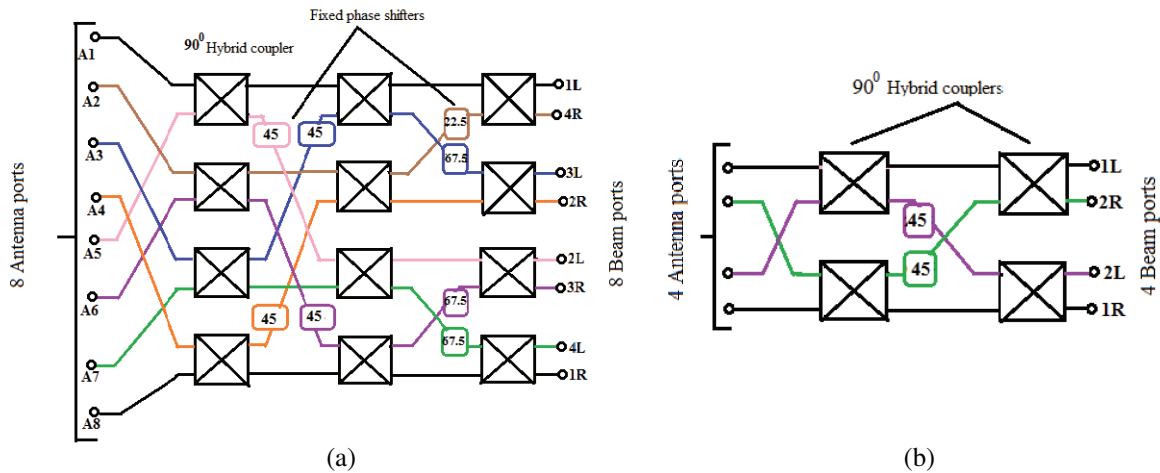
Figure 8. Equivalent DFT algorithm to $Q \times Q$ BM. (a) 8×8 BM to generate eight beams. (b) 4×4 BM to generate four beams.

3.3. Butler Matrix Feeding System

The systematic design procedure of application of BM is described in this section. In this paper, the BM is used to determine the phase shift location and the value in the matrix. The Butler matrix is systematically similar to the DFT algorithm [7, 23]. BM is one of the most beam forming networks used to form multiple beams with linear array, which creates multiple fixed overlapping beams to cover the designated angular area. This matrix is designed in dimensions of 4×4, 8×8 and 16×16 Butler matrices. Based on the dimension of the BM, the directional beams are calculated. For example, a 4×4 BM can form four directional beams. For the generation of five or six beams, the design of BM must be changed, i.e., we have to unport the remaining ports, which is a very difficult task. The designs of the 4×4 and 8×8 BMs using the DFT algorithm are as shown in Figures 8(a) and 8(b). BM generates symmetrical phase locations with respect to input excitations, which are orthogonal to each other. This is the main advantage that helps to choose it for the generation of the multibeam. A 8×8 BM is the combination of 4×4 BMs.

Properties of the BM,

- It is a $N \times N$ passive reciprocal network, hence it is used for both transmission and reception.
- A Butler matrix is isolation between input and output ports, which generates the equal number of inputs and output ports.
- Linearity in phase with respect to the position of output and the increment in phase depends upon the selection of input as symmetric in nature.
- Power fed at input port of Butler matrix is equally divided and is present at all output ports which are given to antenna array.
- Design of BM is similar to DFT algorithm.
- The net field equation for the generation of the multi-beams in Equation (14) is further evaluated till Equation (16), which is equivalent to the mathematical procedure of the DFT algorithm. Hence That a BM is mathematically equivalent to a DFT algorithm is proved.

3.4. Total Field for the Combination of Subarrays

3.4.1. Ideal Situation

In this section, we discuss the design procedure to eliminate the grating lobes. As described in Subsection 3.1, first individual elements are evaluated by a cosine taper method to get the field expression for the multibeam along the horizontal BFC. Since column (linear array) arrays are identical,

we subgrouped Q column (linear array) arrays into a single subarray to generate the Q directional beams. M_s subarrays are formed and combined to free from the grating lobes. The total number of column arrays is $M = M_s Q$ along the horizontal dimension. The length of each subarray is $d_x^b = (Q-1)d_x$, and the total length of such combinational subarrays is $d_x^c = (M_s - 1)d_x^b = (Q-1)(M_s - 1)d_x$. The net field equation for the combination of subarrays using the Equation (7) is given by Equation (12),

$$\bar{E}_\beta = \sum_{b=0}^{M_s - 1} e^{j\Phi_\beta^b} \bar{E}_\beta^b(\bar{r}) \tag{12}$$

where $E_\beta^b(\bar{r})$ is the field equation for each subarray given in Equation (7). In order to get the same main beam direction (i.e., given in Equation (9)) Φ_β^b is given by Equation (13), where $\sin\theta_{peak}^0$ is the direction of the main beam.

$$\Phi_\beta^b = -bd_x k \sin\theta_{peak}^0 \mid_\beta \tag{13}$$

By substituting Equation (7) in (12) we get the net field Equation as follows,

$$\bar{E}_\beta = \bar{E}_0^{c,0}(\bar{r}) \sum_{b=0}^{M_s - 1} \sum_{q=0}^{Q-1} e^{(j\Phi_\beta^b + \Delta\varphi_q^b)} . e^{j2\pi \frac{\beta(q+1)}{Q}} . e^{jk[b+qM_s]d_x \sin\theta} \tag{14}$$

where $\bar{E}_0^{c,0}(\bar{r})$ is the radiation field of the first column array in the subarray. By substituting Equation (13) in Equation (14) we get the following expression, where $\Delta\varphi_q^b$ phase error is practically neglected.

$$\bar{E}_\beta = \bar{E}_0^{c,0}(\bar{r}) e^{j2\pi \frac{\beta}{Q}} \sum_{b=0}^{M_s - 1} \sum_{q=0}^{Q-1} e^{-j2\pi \frac{pb}{M_s}} \tag{15}$$

The above equation is similar to the DFT of the amplitude term $e^{j\Delta\varphi_q^b} = 1$, which is reduced to the equation below,

$$\sum_{b=0}^{M_s - 1} e^{-j2\pi \frac{pb}{M_s}} = \begin{cases} M_s, & q = 0 \\ 0, & \text{otherwise} \end{cases} \tag{16}$$

In Equation (16), the first term indicates the absence of the grating lobe (i.e., $q = 0$ implies the main beam direction), which indicates the null fields at the grating lobes.

3.4.2. General Solution

The above equations are for the ideal case, i.e., absence of grating lobes but practically is not possible, so the Equation (14) can be reformulated as Equation (17), where the column arrays are not equal in general,

$$\bar{E}_\beta = \sum_{b=0}^{M_s - 1} \sum_{q=0}^{Q-1} \left(e^{(j\Phi_\beta^b + \psi_q^\beta)} . e^{j\Delta\varphi_q^b} \bar{E}_q^{c,b}(\bar{r}) \right) \tag{17}$$

where the phase error $\Delta\varphi_q^b$ is negligible, and by substituting Equations (6) and (13) in Equation (17) we get,

$$\bar{E}_\beta(\bar{r}) = \sum_{\tau=0}^{M_b - 1} e^{j\theta_\tau^\beta} E_\tau^c(\bar{r}) \tag{18}$$

where $M_b = M_s Q$ is the total number of column arrays, $\tau = qM_s + b$, and practically the beam forming phase is θ_τ^β and given by,

$$\left. \begin{aligned} \theta_\tau^\beta &= \Phi_\beta^b + \psi_q^\beta \\ &= -bd_x k \sin\theta_{peak}^0 \mid_\beta + 2\pi\frac{\beta(q+1)}{Q} \end{aligned} \right\} \tag{19}$$

4. APPLICATION OF THE SKIRT ELEMENTS

4.1. Beamwidth Control

A $Q \times Q$ BM is used to generate Q directional beams, and the array is subdivided into M_s subarrays to distribute the beams in given coverage domain. To narrow the beam overlapping area and beamwidth, it is desirable to employ redundant skirt antenna elements [24] as shown in Figure 9 (this figure is the setup for eight beam generation, in the case that four beam eight linear arrays are replaced by four linear arrays) to radiate narrow beams. In order to provide the same phase pairs to the skirt elements like core elements, we adopt the concept of amplitude tapering [24] at the edge column arrays (Skirt elements). The skirt elements are placed at the edges only to reduce beam overlapping area. Since the BM is similar to DFT algorithm in functionality, the feeding phases of skirt elements are also same as the core elements as shown in Figure 9, and the feeding phase differences between the core and skirt elements are given by,

$$\Delta \Psi = \begin{cases} 2p\pi; & \text{if } Q \text{ is odd} \\ (2p-1)\pi; & \text{if } Q \text{ is even} \end{cases} \tag{20}$$

These phase differences are called sequential phase pairs, which are generated by the same Butler matrix used at the beamforming circuits. The same phase differences are also maintained at the skirt elements using amplitude tapering. The amplitude tapering provides the excitation to the skirt elements at the edges. So it is desirable to employ the symmetric skirt elements at left and right of the core elements. When skirt elements are included, the field Equation (18) can be extended as follows,

$$\bar{E}_\beta(\bar{r}) = \sum_{\tau=-M_{sk}^l}^{M_b+M_{sk}^r-1} e^{j\theta_\tau^\beta} A_\tau E_\tau^c(\bar{r}) \tag{21}$$

where M_{sk}^l and M_{sk}^r are the skirt elements on the left and right sides respectively as shown in Figure 9, and A_τ is the amplitude tapering weight. The phase term θ_τ^β is expressed in Equation (19). $\tau = qM_s + b$, where $0 \leq b \leq M_s - 1$, number of the subarrays. The term A_τ is amplitude weight provided by power divider by satisfying the power conservation of ideal power divider given by Equation (22),

$$\sum_{\mu=-M_{sk,l}^{b,q'}}^{M_{sk,r}^{b,q'}} \mid A_{\mu(QM_b)+q'M_s+b} \mid^2 = 1 \tag{22}$$

where $0 \leq q' \leq Q$ represents the number of column arrays in the given bth subarray. The left and right hand limits $(M_{sk,l}^b, M_{sk,r}^b)$ are decided by selecting the elements of (q', b) in the original array first, then finding the left most and right most elements of the arrangement as shown in Figure 9. The number of skirt elements needed are calculated by using a normalized gain formula at the intersecting point of the
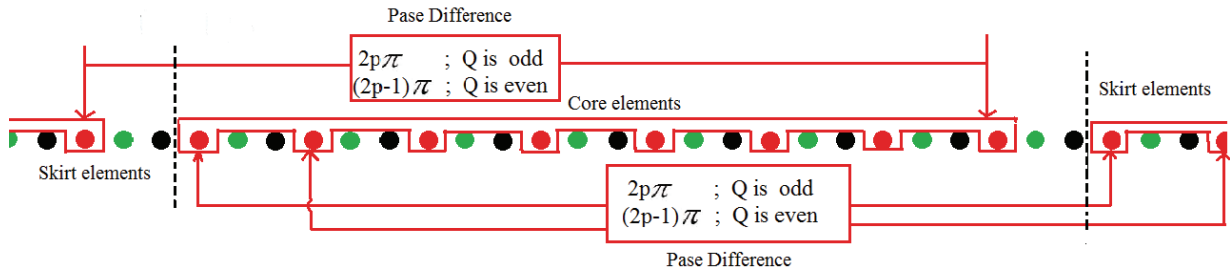

Figure 9. Inclusion of Skirt elements to control beamwidth and narrowing beam overlapping for case study: 1.

two adjacent beams, which is given by equation

$$G_{norm} = \frac{(\widehat{e}.\bar{E}_0^{c,b}(\theta_{bw}))}{(\widehat{e}.\bar{E}_0^{c,b}(\theta = 0))} \frac{\sin\left(\frac{\pi(M_b + M_{sk}^l + M_{sk}^r)}{2M_b}\right)}{(M_b + M_{sk}^l + M_{sk}^r)\sin\left(\frac{\pi}{2M_b}\right)} \tag{23}$$

where $\widehat{e}$ is the unit vector corresponding to copolarization, and the term θ_{bw} is derived from Equation (11) as $\sin\theta_{bw} = \lambda/(2Qd_x^b)$. G_{norm} is given by user to M_{sk}^l and M_{sk}^r.

4.2. Numerical Case Study

- The linear phase excitations (phase difference) from the 4×4 BM in Table 3 are given by Equation (6), where the first term is the DFT liner phase obtained from BM. The second term is the phase error, which is neglected in practice.
- The beam indicator β is given by'

$$\beta = \left\{ \begin{array}{ll} \pm\left(\frac{1}{2}, \frac{3}{2}, \frac{5}{2} \ldots\right), & \text{for } Q = \text{even} \\ \pm(1, 2, 3 \ldots), & \text{for } Q = \text{odd} \end{array} \right\}$$

- For a better understanding, an example for the phase calculation of the 4×4 uses Equation (6) and above β condition, where Q is even, i.e., four. Four symmetrical phases are obtained, i.e., four values of β are $\pm\frac{1}{2}$ and $\pm\frac{3}{2}$ substituted in Equation (6) for four values of q receptively. The BM matrix phases are ψ_q^b as $-\frac{\pi}{4}, \frac{3\pi}{4}, -\frac{3\pi}{4}$ and $\frac{\pi}{4}$, respectively.
- The maximum beam direction angles obtained in Table 3 are calculated with Equation (9) using the above four β values and by substituting the $d_x^b = \lambda/2$ in Equation (9), then the beam angles are calculated as $-15°, -40°, 40°$ and $15°$, respectively.
- The normalized gain at the intersection of the two adjacent beams is fixed as -12 dB refereed from [24] and substituted in Equation (23).
- Where $\bar{E}_0^{c,b}(\theta_{bw})$ is same for all the beams and calculated at $\theta_{bw} = \lambda/(2Qd_x^b) = \lambda/(2*4*\lambda/2) = 1/8$ and also repeated at $\theta_{bw} = 0$ and substituted in Equation (23).
- Equation M_b in terms of skirt elements M_{sk}^l and M_{sk}^r is generated.
- Also the condition in Eq. (22) is checked to get M_b in terms of skirt elements M_{sk}^l and M_{sk}^r.
- The above two equations are solved to eliminate M_b, and the number of skirt elements is obtained as four ($M_{sk}^r = M_{sk}^r = 2$) for the case of four-beam generation.
- Similarly for the case of eight beams, the number of skirt elements is calculated as six ($M_{sk}^r = M_{sk}^r = 3$) by equating the normalized gain Equation (23) to the fixed value of -12 dB.

Table 3. Phase distribution of a 4×4 Butler matrix feed.

Beam port/ Ant port	A1	A2	A3	A4	Phase diff (deg)	Beam angle (deg)
Beam 1 (1L)	-45	-90	-135	-180	-45	-15
Beam 2 (2L)	-135	0	$135/-225$	$270/-90$	135	-40
Beam 3 (2R)	-90	$-135/225$	0	-135	-135	40
Beam 3 (1R)	-180	-135	-90	-45	45	15

4.3. Amplitude Tapering

The amplitude weights A_τ are expressed as cosine functions symmetrically given in Table 4 [24], where the first column (when $\mu = 0$) of the table indicates the original array, i.e., without skirt elements with index of the element $\xi = q'M_s + b$. The terms of the second column of Table 4 are the elements of the skirt columns, indicated by $\mu \neq 0$. The corresponding amplitudes are calculated by multiplying their respective columns of the table and then splitting the energy equally for both sides of the skirt elements. These calculations will satisfy Equation (22). Practically, the original basic array will get a smooth amplitude distribution because of the first term $\cos\theta_0^\xi$ in the table, where $0 \leq \theta_0^\xi \leq \pi/2$ is the smallest, which increases for outermost elements (i.e., for skirt elements). The complexity of the BM is calculated based on the DFT algorithm, where we have used $Q \times Q$ BM to generate the Q directional beams with a complexity of $Q\log_2 Q$. On the other hand, M_s subgroups are considered with a complexity of $M_sQ\log_2 Q$. The number of power dividers used is $M - M_sQ$, so the total complexity is $M_sQ\log_2 Q + M - M_sQ = M + (\log_2 Q - 1)M_sQ$.

Table 4. Alternative representation of the amplitude tapers, which assures Equation (23) to be satisfied.

$\mu = 0$	$\mu = \pm\mu_1$	$\mu = \pm\mu_2$	$\mu = \pm\mu_3$	$\mu = \pm\mu_4$	$\mu = \pm\mu_4$
$\cos\theta_0^\xi$	$\sin\theta_0^\xi$	$\sin\theta_0^\xi$	$\sin\theta_0^\xi$	$\sin\theta_0^\xi$	$\sin\theta_0^\xi$
	$\cos\theta_1^\xi$	$\sin\theta_1^\xi$	$\sin\theta_1^\xi$	$\sin\theta_1^\xi$	$\sin\theta_1^\xi$
		$\cos\theta_2^\xi$	$\sin\theta_2^\xi$	$\sin\theta_2^\xi$	$\sin\theta_2^\xi$
			$\cos\theta_3^\xi$	$\sin\theta_3^\xi$	$\sin\theta_3^\xi$
				$\cos\theta_4^\xi$	$\sin\theta_4^\xi$

5. PROPOSED METHOD WITH DESIGN SPECIFICATIONS

The proposed method is experimented on various case studies, and the results are explained in this section. $Case1$ is for eight beams, $Case2$ for four beams, and $Case3$ for six beams. To achieve this, the planner sizes are fixed to 8×12 in $case1$ and 4×8 in $Case2$ with antenna elemental spacing $d_x = \lambda/2$. The feeding circuits for the fixed planner sizes are 8×8 BM and 4×4 BM, respectively. The antenna elements are given with complex excitations. The amplitude of the complex excitations are from the cosine tapers Equation (1) considering the ideal situation $t_1 = t_2 = 0$. The linear phase is given by the Butler matrix. The pattern generated from a single column (linear array) using cosine tapers is given in Figure 10 for eight beam generation. For generating multiple beams in the referred plane, different interleaved columns (linear arrays) are grouped. Further the beam overlapping area can be reduced by using skirt elements. The cosine tapers excitations help in reduction of elemental patterns at wide angles. For example, 10 dB is the threshold to define a coverage domain, then the generated multiple beams can be roughly fitted into a span of 70°. If the threshold further decreases, the angular span will not be sufficient to cover multiple beams in prescribed angular area, hence it leads to abandoning the multiple beams outside the coverage domain. The grouping is done as per Equation (4) to generate the multiple beams. All the computations are worked out on processor, intel(R)core(TM)i5-2000 CPU@3.10 GHz, RAM with 4 GB and Matlab R2014a(8.1.0.604).

5.1. Case Study: 1 Generation of Eight Beams

In this case, an 8×12 array is used to generate eight beams, where eight interleaved columns, which contain 12 elements in each column, are grouped. The elements in each column array are analyzed by using cosine tapers, and each column array is represented by a field equation given in Equation (4), and the radiation pattern is as shown in Figure 10, where the blue line indicates the 0 dB line. Thus the eight column arrays are grouped with a spacing of $d_x^b = 7d_x$ since Figure 11 shows an eight-beam radiation pattern with grating lobes at wider angles. The directional beams are generated from an 8×8 BM as shown in Figure 8(a). The BM employs DFT algorithm to generate linear phases for the grouped arrays
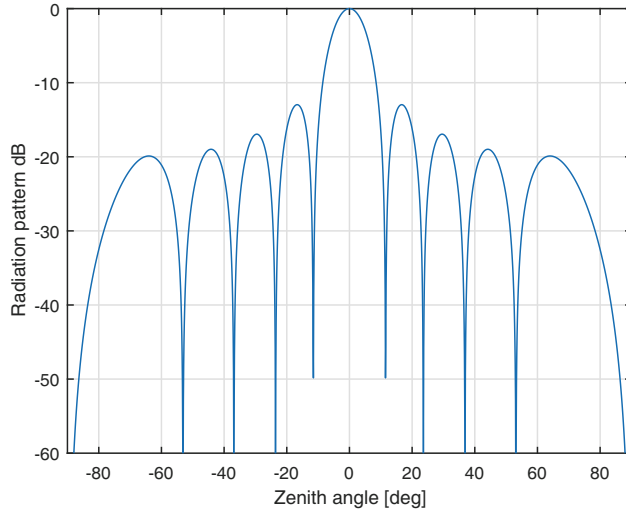
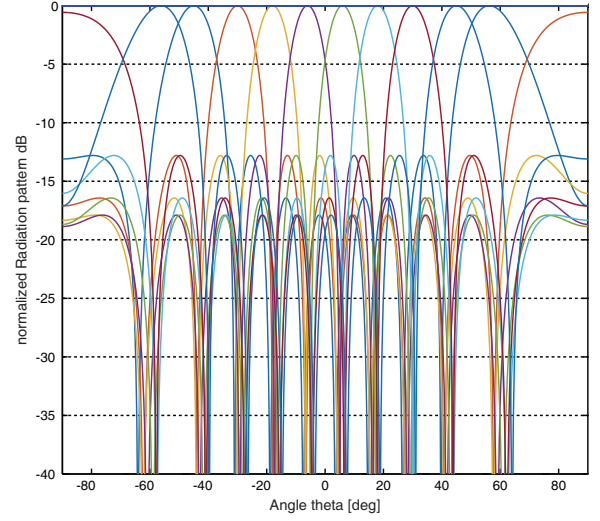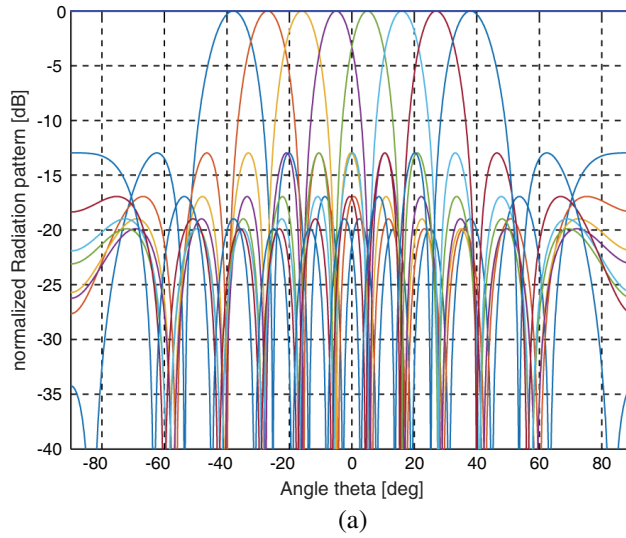**Figure 10.** Radiation pattern of single column array with 12 antenna elements.
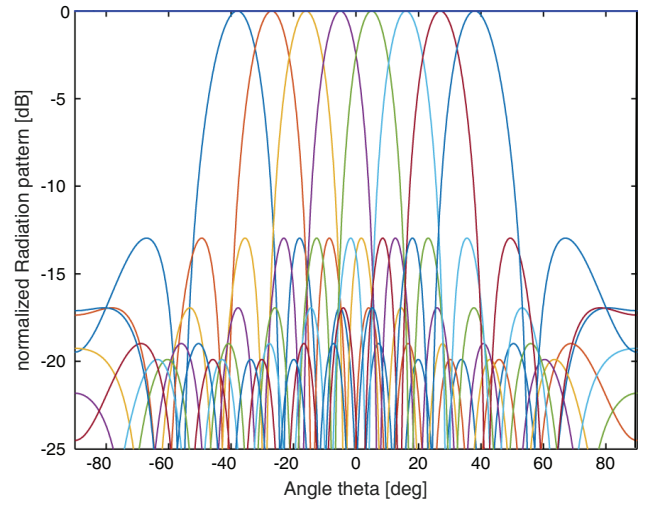

Figure 11. Radiation pattern of subarray of eight columns with grating lobes.

(a)

(b)

Figure 12. Radiation pattern of 8 beams by combination of two sub arrays for reduction of grating lobes. (a) Radiation pattern using array factor. (b) Radiation pattern using elemental pattern.

which are tabulated in Table 2. The grating lobes levels at wider angles are reduced by appending such subarrays with same excitations by same BM using Equation (17). The phases of appended beams are orthogonal to each other hence cancel out the grating lobes, which is reflected in Figure 12(a). The grating lobes are efficiently suppressed in Figure 12(b) compared to Figure 12(a) because of considering cosine tapers instead of array factor without change in beam direction and beamwidth. The gain levels at the intersecting points are 4 dB below the peaks, which indicates a large overlapping area. The reduction in the overlapping area of multiple beams can be enhanced by using skirt elements as explained in Section 4. The number of skirt elements required is decided by fixing the normalized gain as -12 dB [24] and equating it to Equation (23), which results in four skirt elements required for this case. The introduction of skirt elements along with core array elements results in even number of arrays as shown in Figure 14, which leads to phase angle of π radian as given in Equation (20). The radiation pattern using skirt elements is as shown in Figure 13(a) by using array factor and in Figure 13(b) using
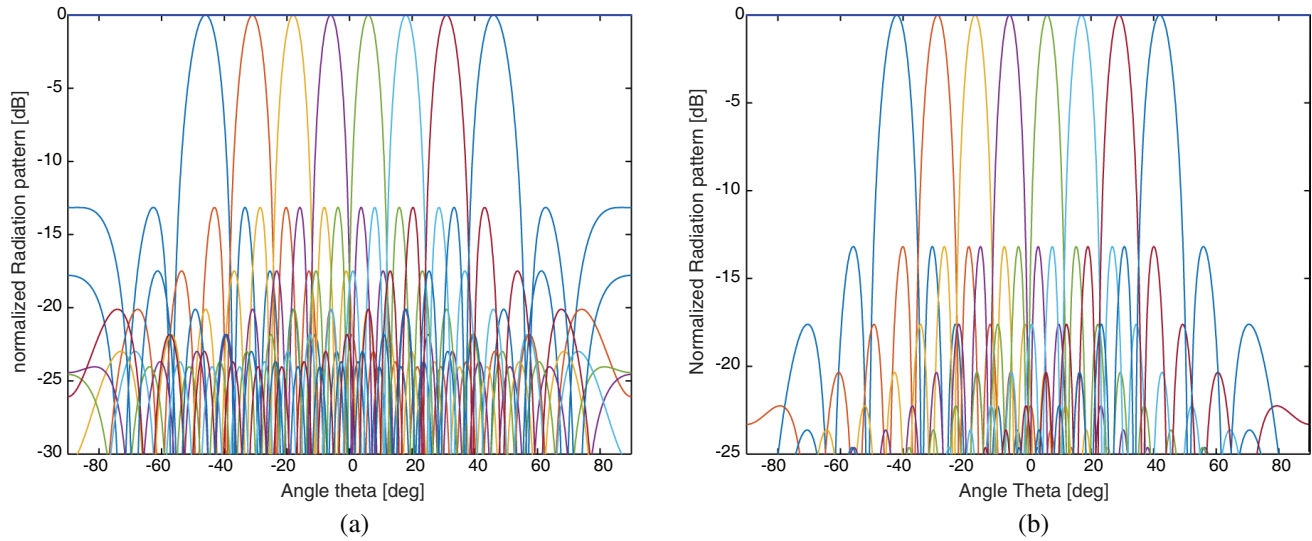
Figure 13. Reduction of beam overlapping area with skirt elements foe eight beams. (a) Radiation pattern using array factor. (b) Radiation pattern using elemental pattern.
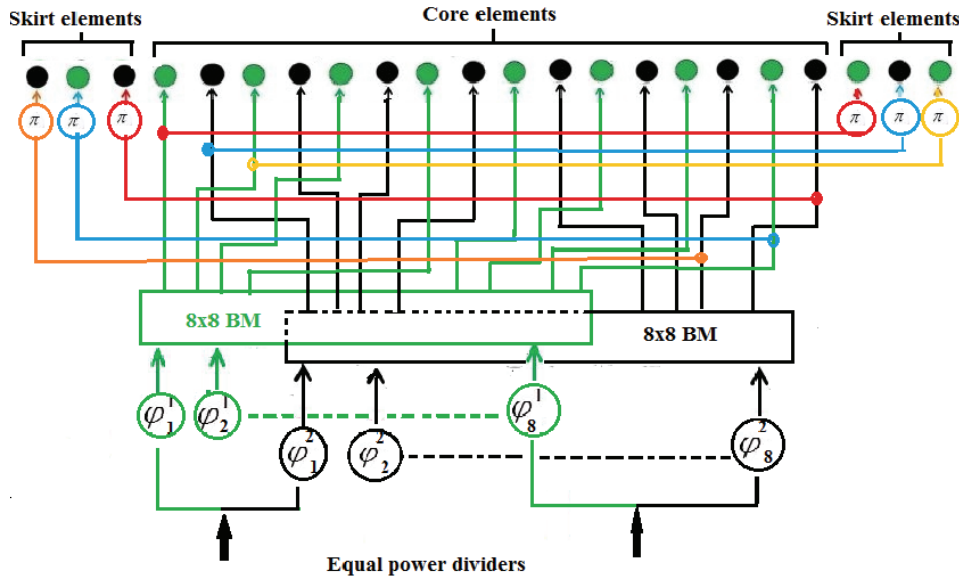

Figure 14. Inclusion of six skirt elements to Figure 7 for narrowing beamwidth and reducing beam overlapping for case study:1.

cosine tapers. In order to give the same excitation to the skirt elements, amplitude tapering is adopted as explained in Subsection 4.3, where one can observe that the first column (linear array) array in core part and the seventeenth column array (i.e., the first column array in the right side skirt arrays) share the same power and phase as shown in Figure 14. By using skirt elements, the beam overlapping area and beamwidth are reduced in Figures 13(a) and 13(b) as compared Figures 12(a) and 12(b), respectively. When the number of columns (linear arrays) grouping to subarray increases, the need of skirt elements decreases, but the complexity of the BM increases.

5.2. Case Study: 2 Generation of Four Beams

In this case, an 4×8 array is used to generate the four beams, where four interleaved columns, which contain 8 elements in each column, are grouped. The elements in each column array are analysed by using cosine tapers, and each column array is represented by a field equation given in Equation (4), and the radiation pattern is as shown in Figure 15. Thus the four column arrays are grouped with a spacing of $d_x^b = 3d_x$. Figure 16 shows a four-beam radiation pattern with grating lobes at wider angles. The directional beams are generated from a 4×4 BM as shown in Figure 8(b). The BM employs DFT algorithm to generate linear phases for the grouped arrays, tabulated in Table 3. The grating lobes at wider angles are reduced by appending such subarrays with same excitations by BM using Equation (17). The phases of appended beams are orthogonal to each other hence cancel out the grating lobes which is reflected in Figure 17. The gain levels at the intersecting points are 4 dB below the peaks, which indicates a large overlapping area. The reduction in the overlapping area of multiple
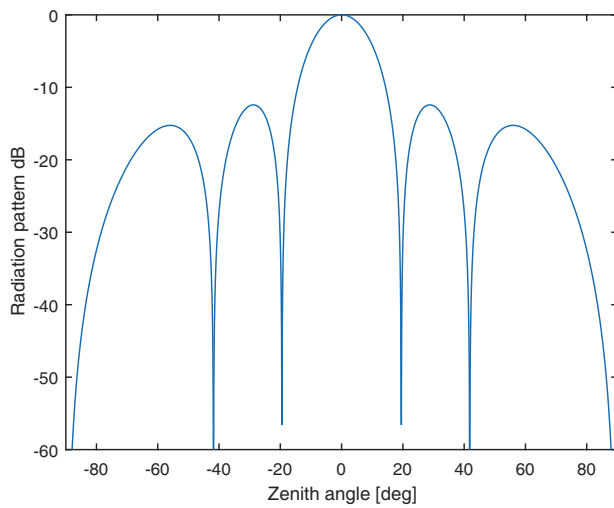

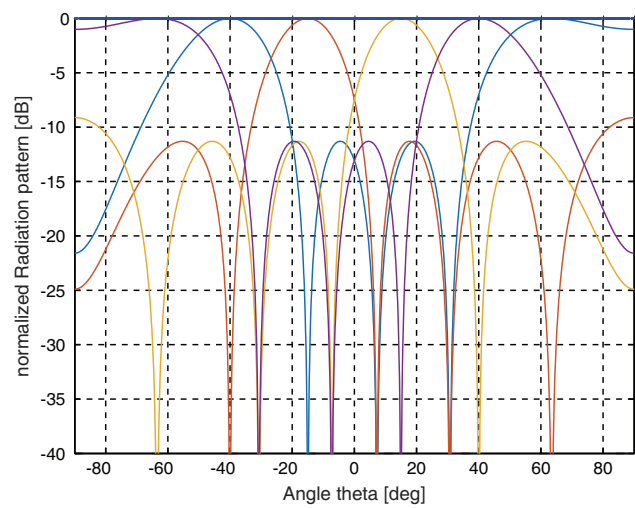**Figure 15.** Radiation pattern of single column array with eight antenna elements.

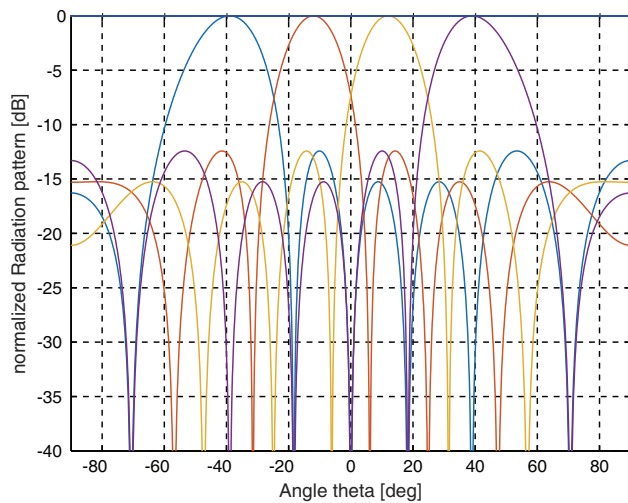**Figure 16.** Radiation pattern of four beams with grating lobes.

Figure 17. Radiation pattern of four beams by combination of two subarrays for reduction of grating lobes.
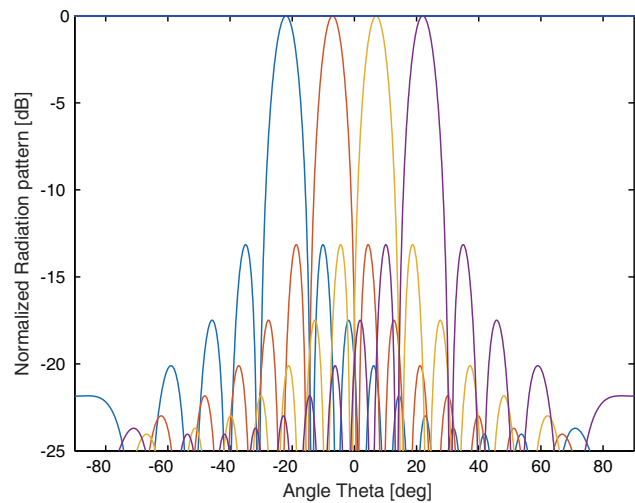

Figure 18. Radiation pattern of four beams for reduction of beam overlapping using skirt elements.

beams can be enhanced by using skirt elements as explained in Section 4. The number of skirt elements required is decided by fixing the normalized gain as -12 dB [18] and equating it to Equation (23), which results in six skirt elements required for this case. The introduction of skirt elements along with core array elements results in even number of arrays as shown in Figure 14 (This figure is also used for four elements if we replace eight elements by four), which leads to phase angle of π *radian* as given in Equation (20). The radiation pattern using skirt elements is as shown in Figure 18. In order to give the same excitation to the skirt elements, amplitude tapering is adopted as explained in Subsection 4.3, where one can observe that the first column array (linear array) in core part and the third column array (i.e., the first column array in the right side skirt arrays) share the same power and phase as shown in Figure 14. By using skirt elements, the beam overlapping area and beamwidth are reduced in Figure 18 compared to Figure 17. If -10 dB is taken as the threshold to define the coverage domain, it is roughly $\pm 70°$, representing a large angular span. To narrow down the coverage domain, one may use the central two beams and abandon the outer two beams by placing perfect loads in the corresponding two beam ports.
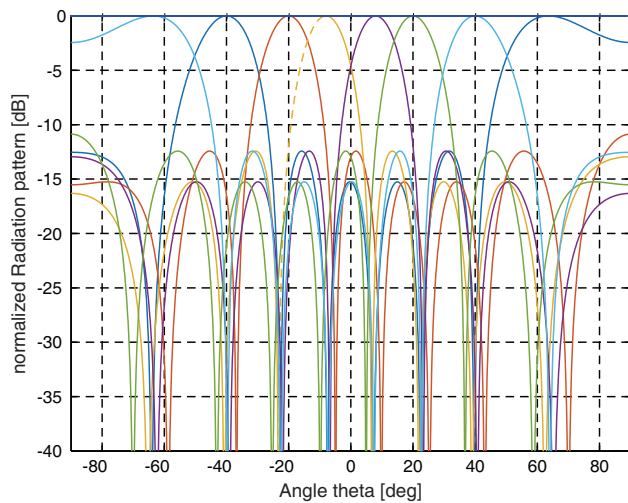

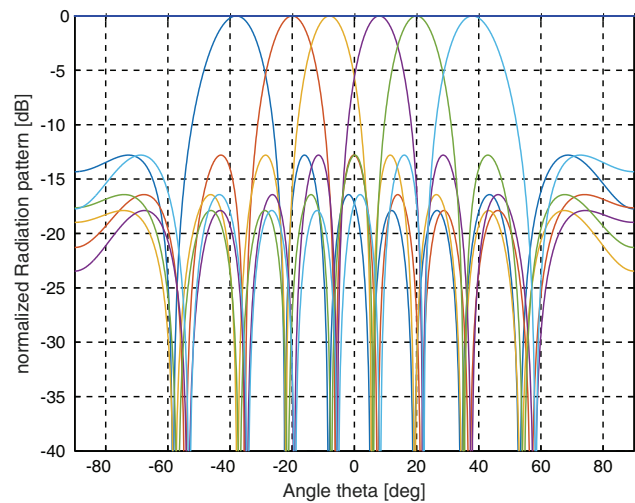**Figure 19.** Radiation pattern of six beams with grating lobes.

Figure 20. Radiation pattern of six beams without grating lobes.
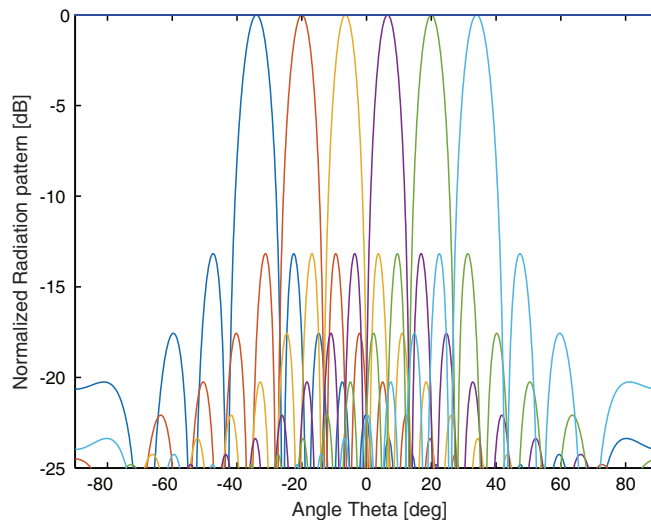

Figure 21. Radiation pattern of six beams for reduction of beam overlapping using skirt elements.

5.3. Case Study 3: Generation Six Beam

This is a special case of eight beam generation, where the right most and one left most ports of an 8×8 BM are switched off to form only six beams as shown in Figure 19. Remaining procedure for the reduction of grating lobes and beam overlapping area is the same for both the cases. The radiation patterns are as shown in Figures 20 and 21. However, it is very difficult in the design of BM to generate only six beams. In this case, same number of skirt elements are also required to reduce the beam overlapping area.

6. CONCLUSION

This paper presents the design methodology of multibeam using phased array. BFC circuits are employed to form field basis for multiple beams using BM. The directional beams from the BM are liner in phase and uniform. Further, the beamwidth and overlapping area are controlled by method of skirt elements. The current work is applicable to the design of antennas for uniformly spaced multiple beams, which is beneficial in multisattilite and mobile communications. If two adjacent beams can be combined using unequal power ratio to create a beam in arbitrary directions within the coverage of these two beams, the BFC complexity will be increased. The future work can attempt a study on feeder synthesis with least circuit complexity.

REFERENCES

1. Schulwitz, L. and A. Mortazawi, "A compact dual-polarized multibeam phased-array architecture for millimeter-wave radar," *IEEE Trans. Microw. Theory Techn.*, Vol. 53, No. 11, 3588–3594, Nov. 2005.
2. Jacomb-Hood, A. and E. Lier, "Multibeam active phased arrays for communications satellites," *IEEE Microw. Mag.*, Vol. 1, No. 4, 40–47, Dec. 2000.
3. Wang, J., Y. Fang, and D.-P.Wu, "Enhancing the performance of medium access control for WLANs with multi-beam access point," *IEEE Trans. Wireless Commun.*, Vol. 6, No. 2, 556–565, Feb. 2007.
4. Chou, Z.-T., C.-Q. Huang, and J. M. Chang, "OoS provisioning for wireless LANs with multi-beam access point," *IEEE Trans. Mobile Comput.*, Vol. 13, No. 9, 2113–2127, Sep. 2014.
5. Fonseca, N. J. G. and J. Sombrin, "Multi-beam reflector antenna system combining beam hopping and size reduction of effectively used spots," *IEEE Antennas Propag. Mag.*, Vol. 54, No. 2, 88–89, Apr. 2012.
6. Chou, H.-T., "An efficient synthesis approach for electromagnetic nearand far-field contoured patterns using alternative narrow-beam field functions transformed from the radiations of linearly excited array antennas with least computational complexity," *Radio Sci.*, Vol. 50, No. 5, 365–380, 2015.
7. Moody, H., "The systematic design of the Butler Matrix," *IEEE Transactions on Antennas and Propagation*, Vol. 12, No. 6, 786–788, Nov. 1964.
8. Denidni, T. A. and T. E. Libar, "Wide band four-port Butler Matrix for switched multibeam antenna arrays," *Proc. IEEE Pers., Indoor, Mobile Radio Commun.*, Vol. 3, 2461–2464, Sep. 2003.
9. Kozuki, Y. and H. Arai, "Layered Butler Matrix circuit for vertical multi beam of cellular base station antenna," *Proc. Int. Symp. Antennas Propag.*, 561–562, Dec. 2014.
10. Mosca, S., F. Bilotti, A. Toscano, and L. Vegni, "A novel design method for Blass matrix beam-forming networks," *IEEE Transactions on Antennas and Propagation*, Vol. 50, No. 2, 225–232, Feb. 2002.
11. Varghese, K. J., A. K. Singh, and S. Christopher, "Experimental characterisation of Moreno cross slot couplers for Blass matrix design," *Defence Sci. J.*, Vol. 48, No. 4, 413–416, 2013.
12. Neto, A., M. Ettorre, G. Gerini, and P. De Maagt, "Leaky wave enhanced feeds for multibeam reflectors to be used for telecom satellite based links," *IEEE Transactions on Antennas and Propagation*, Vol. 60, No. 1, 110–120, Jan. 2012.

13. Fujita, M., K. Takano, S. Tanaka, Y. Utsumi, and T. Murata, "Experimental results on multi-beam receiving antenna for satellite broadcasting," *Proc. IEEE Int. Symp. Phased Array Syst. Technol.*, 117–120, May 2000.

14. Ramanujam, P. and L. R. Fermelia, "Recent developments on multi-beam antennas at Boeing," *Proc. 8th Eur. Conf. Antennas Propag. (EuCAP)*, 405–409, Apr. 2014.

15. Ebling, J. P., G. M. Rebeiz, and B. Schoenlinner, "Multi-beam antenna," U.S. Patent 7 042 420, May 9, 2006.

16. Thornton, J., A. White, and D. Gray, "Multi-beam lens-reflector for satellite communications: Construction issues and ground plane effects," *Proc. 3rd Eur. Conf. Antennas Propag. (EuCAP)*, 1377–1380, Mar. 2009.

17. Zhang, Y. S. and W. Hong, "A millimeter-wave gain enhanced multibeam antenna based on a coplanar cylindrical dielectric lens," *IEEE Transactions on Antennas and Propagation*, Vol. 60, No. 7, 3485–3488, Jul. 2012.

18. Van Veen, B. D., D. Barry, and K. M. Buckley, "Beamforming: A versatile approach to spatial filtering," *IEEE ASSP Magazine*, Vol. 5, No. 2, 4–24, 1988.

19. Rahmat-Samii, Y. and S.-W. Lee, "Directivity of planar array feeds for satellite reflector applications," *IEEE Transactions on Antennas and Propagation*, Vol. 31, No. 3, 463–470, May 1983.

20. Wang, J., Y. Fang, and D.-P.Wu, "Enhancing the performance of medium access control for WLANs with multi-beam access point," *IEEE Trans. Wireless Commun.*, Vol. 6, No. 2, 556–565, Feb. 2007.

21. Chou, Z.-T., C.-Q. Huang, and J. M. Chang, "OoS provisioning for wireless LANs with multi-beam access point," *IEEE Trans. Mobile Comput.*, Vol. 13, No. 9, 2113–2127, Sep. 2014.

22. Ueno, M., "A systematic design formulation for Butler Matrix applied FFT algorithm," *IEEE Transactions on Antennas and Propagation*, Vol. 29, No. 3, 496–501, May 1981.

23. Sheltont, J. P. and K. S. Kelleherz, "Multiple beams from linear arrays," *IRE Transaction on Antennas and Propagation*, Vol. 9, No. 2, 154–161, 1961.

24. Chou, H.-T., "An Effective design procedure of multibeam phased array antennas for multisatellite communications," *IEEE Transactions on Antennas and Propagation*, Vol. 64, No. 10, 4218–4227, October 2016.

25. Yazdanbakhsh, P. and K. Solbach, "Microstrip Butler Matrix design and realization for 7 T MRI," *Magnetic Resonance in Medicine*, Vol. 66, No. 1, 270–280, 2011.

26. Khan, O. U., "Design of X-band 4×4 Butler Matrix for microstrip patch antenna array," *TENCON 2006, 2006 IEEE Region 10 Conference*, IEEE, 2006.

27. Alam, M. M., "Microstrip antenna array with four port Butler Matrix for switched beam base station application," *12th International Conference on Computers and Information Technology, 2009, ICCIT'09*, IEEE, 2009.

28. Fakoukakis, F. E., et al., "Design and implementation of Butler matrix-based beam-forming networks for low sidelobe level electronically scanned arrays," *International Journal of Microwave and Wireless Technologies*, Vol. 7, No. 1, 69–79, 2015.

29. Muhammad, N. A., et al., "Beam forming networks using reduced size Butler Matrix," *Wireless Personal Communications*, Vol. 63, No. 4, 765–784, 2012.

30. Zhai, Y., et al., "Miniaturization design for 8×8 Butler matrix based on back-to-back bilayer microstrip," *International Journal of Antennas and Propagation*, Vol. 2014, 2014.

31. Fonseca, N. J. G., "Printed S-band 4×4 nolen matrix for multiple beam antenna applications," *IEEE Transactions on Antennas and Propagation*, Vol. 57, No. 6, 1673–1678, 2009.

32. Garcia-Rodriguez, A., et al., "Hybrid analog-digital precoding revisited under realistic RF modeling," *IEEE Wireless Communications Letters*, Vol. 5, No. 5, 528–531, 2016.

33. Jayakrishnan, V. M. and S. K. Menon, "Realization of butlermatrix for beamforming in phased array system," *Procedia Computer Science*, Vol. 93, 223–229, 2016.